ELSEVIER

NeuroImage

www.elsevier.com/locate/ynimg
NeuroImage 25 (2005) 122–132

CASL fMRI of subcortico-cortical perfusion changes during memory-guided finger sequences

Gaëtan Garraux,[a,b] Mark Hallett,[a,*] and S. Lalith Talagala[c]

[a]*Human Motor Control Section, National Institute of Neurological Disorders and Stroke, National Institutes of Health, Building 10, Room 5N226, 10 Center Dr., MSC 1428, Bethesda, MD 20892-1428, USA*
[b]*Cyclotron Research Center and Department of Neurology, University of Liège, Sart Tilman B30, 4000, Liège, Belgium*
[c]*NIH MRI Research Facility, National Institute of Neurological Disorders and Stroke, National Institutes of Health, Bethesda, MD 20892-1428, USA*

Received 28 June 2004; revised 5 October 2004; accepted 2 November 2004
Available online 5 January 2005

Arterial spin labeling (ASL) perfusion functional magnetic resonance imaging (fMRI) is an attractive alternative to BOLD fMRI. Nevertheless, current ASL fMRI techniques are limited by several factors that hamper more routine applications in humans. One of these factors is restricted brain coverage so that whole-brain ASL fMRI studies have never been reported. The present study tested the ability of a multislice continuous ASL (CASL) fMRI approach using a small surface coil placed on the subject's neck to map changes in regional cerebral blood flow (rCBF) throughout the brain while healthy individuals (N = 15) performed memory-guided sequential finger movements at a mean rate of ~0.5 Hz. As predicted by results from a large number of studies, reliable task-related increases in flow were detected across subjects not only in primary and associative cortical areas but also in subcortical brain regions. When normalized to baseline, rCBF increased 31% in the hand representation area (HRA) of left primary motor cortex (M1), 13% in the left supplementary motor area proper (SMA), 10% in the left dorsolateral prefrontal cortex (DLPFC), 10–18% in the bilateral intraparietal sulci, 6% in the HRA of left putamen, 10% in the left thalamus, and 17% in the right anterior cerebellum. In addition to these increases, 6% and 4% decreases in rCBF were detected in the HRA of the right M1 and the bilateral posterior cingulate sulci, respectively. These results demonstrate that perfusion-based fMRI using CASL with a separate labeling coil can now be used to characterize task-related flow changes in most of the brain volume with adequate accuracy and sensitivity.
Published by Elsevier Inc.

Keywords: Cerebral blood flow; Arterial spin labeling; fMRI; Motor system; Deactivation

Introduction

Cerebral blood flow (CBF), the rate of delivery of blood to a local tissue volume, is a fundamental marker of human brain function in health and disease, and is also used as an index for mapping functional neuroanatomy. Many different magnetic resonance imaging (MRI) techniques using exogenous or endogenous tracers have been developed to image various parameters related to CBF (Barbier et al., 2001). Arterial spin labeling (ASL) MRI refers to a group of noninvasive techniques using magnetically labeled arterial water ^{1}H spins as an endogenous tracer for measuring CBF (Detre et al., 1992; Williams et al., 1992). In ASL, the state of blood water magnetization is modified in an artery proximal to the tissue of interest. After a delay that is long enough to permit arrival at the capillary site, the labeled water exchanges with interstitial and intracellular water. This elicits a local change in longitudinal tissue magnetization. The magnitude change in magnetization due to labeling is proportional to CBF and other measurable parameters and is determined by subtraction of images acquired with arterial spin labeling from images acquired without labeling (control images).

ASL can be used to monitor changes in regional CBF (rCBF) that correlate with rapid changes in behavior, and, indeed, various ASL techniques have been successfully used for functional MRI (fMRI) experiments in healthy individuals (Buxton et al., 1998; Edelman et al., 1994; Kim, 1995;Talagala and Noll, 1998; Wong et al., 1997; Ye et al., 1997; Yongbi et al., 2002). For this purpose, the ASL signal presents several potential advantages over BOLD contrast. Signal changes detected using ASL might be more closely related to variations in neuronal activity because ASL MRI is sensitive to the arterial side of the vascular tree, in particular, the capillaries. Therefore, ASL can better localize functionally active sites while BOLD can be influenced by signal changes in draining veins (Duong et al., 2001). Whereas BOLD is still a qualitative technique, quantification in well-characterized units of ml 100 g^{-1} min^{-1} can be obtained using ASL fMRI. This may be particularly

* Corresponding author. Fax: +1 301 480 2286.
E-mail address: hallettm@ninds.nih.gov (M. Hallett).
Available online on ScienceDirect (www.sciencedirect.com).

1053-8119/$ - see front matter. Published by Elsevier Inc.
doi:10.1016/j.neuroimage.2004.11.004

important for meaningful interpretation of results from longitudinal and pharmacological fMRI experiments as well as studies comparing normal and patient populations. Furthermore, evidence to date suggests the absence of temporal autocorrelation in ASL time series, making perfusion-based fMRI a method of choice to test some hypotheses (Wang et al., 2003a).

However, current ASL fMRI techniques are limited by several factors that hamper more routine applications in humans. In addition to lower sensitivity and temporal resolution compared to BOLD, an important limiting factor is the extent of the imaging region. Although multislice ASL imaging covering much of the brain has been demonstrated (Wang et al., 2002), extension of ASL imaging to also cover lower brain regions and cerebellum is generally accompanied by reduced labeling efficiency when using the same RF coil for imaging and labeling. This compromises the perfusion image signal-to-noise ratio (SNR) in all brain regions.

In this regard, continuous ASL (CASL) perfusion MRI with a separate labeling coil is attractive for whole-brain human studies (Silva et al., 1995; Zaharchuk et al., 1999; Zhang et al., 1995). In this approach, a small surface coil is placed on the neck of the subject to invert the magnetization of the blood flowing in the carotid and vertebral arteries, providing a good labeling efficiency for all major arteries. Unlike methods using the same RF coil for labeling and imaging, magnetization transfer (MT) effects are completely eliminated using a two-coil system and RF power deposition due to spin labeling is reduced and restricted to the immediate vicinity of the labeling coil. Recently, Talagala et al. (2004a) demonstrated that this approach can indeed be used safely in humans to measure resting state CBF with good SNR in the whole brain and without exceeding the current RF power deposition limits. However, since the images were acquired using a 3D sequence requiring a relatively long scan time (~48 s/volume), the image acquisition method used in that study is not directly suitable for most fMRI applications. A more adequate temporal resolution can be achieved with single-shot 2D echo planar imaging (EPI). It is important to emphasize that, since MT effects are absent in ASL fMRI using a two-coil system, individual slices can be acquired anywhere and in any orientation within the brain (Talagala et al., 2004a; Zaharchuk et al., 1999). A disadvantage of 2D compared to 3D acquisitions for whole brain ASL studies is that the slices acquired later show reduced SNR due to perfusion signal decay during the interval between labeling and slice acquisition.

Therefore, the goal of the present study is to test whether or not CASL with a separate labeling coil combined with a 2D EPI imaging could provide adequate SNR in all slices to enable fMRI studies throughout the brain in healthy individuals. CASL fMRI using a separate labeling coil has been demonstrated recently (Mildner et al., 2003). However, that study was restricted to detecting perfusion only in the right hemisphere and, moreover, only four slices covering the most superior aspect of the brain were studied. In the present study, increases and decreases in rCBF were monitored as healthy individuals performed alternating blocks of memory-guided, visually triggered sequential finger movement and visual control conditions (baseline). Based on results from a large number of whole-brain $H_2^{15}O$-PET and BOLD fMRI studies that used a similar task paradigm (Catalan et al., 1998; Colebatch et al., 1991; Grafton et al., 1995; Haslinger et al., 2002; Menon et al., 2000; Sadato et al., 1996; Sakai et al., 1998), we predicted a relative increase in activity in the frontoparietal areas and basal ganglia predominant in the hemisphere contralateral to the moving hand, as well as in the ipsilateral cerebellar hemisphere. We also expected to observe a relative decrease in flow during the active task in medial parietal areas (Raichle et al., 2001) and in the hand representation area (HRA) of the primary sensorimotor cortex (S1M1) ipsilateral to the moving hand (Allison et al., 2000).

Methods

Subjects

Informed verbal and written consent for this research protocol, which was approved by the NINDS Institutional Review Board, was obtained from all subjects. Fifteen healthy subjects (seven females) aged between 21 and 40 years (mean age 29 years) were recruited from the NIH database of volunteers. All participants were right handed according to the Edinburgh Inventory (Oldfield, 1970). None of them had any history of neurological disorder, head trauma with loss of consciousness, epilepsy, brain surgery, systemic illness, excessive drug or alcohol consumption.

Task procedures

Subjects lay supine in the scanner and wore nonmagnetic prism glasses allowing them to comfortably see an opaque screen located at their feet and on which visual stimuli and a fixation point were rear projected. A vacuum bag was used to reduce head movements during image acquisition. The right hand rested on an ergonomic right hand five-button response unit (MRI devices corporation, Waukesha, WI, USA). There was a one-to-one mapping between a digit and a key.

The experiment was organized according to a blocked design. An fMRI time series included six cycles of three blocks. The first block of each cycle lasted 12 s whereas the two last blocks lasted 48 s. The onset of each block condition was indicated to the subjects by displaying a short instruction on the screen for 400 ms: ‘sequence’, ‘movement’, and ‘fixation cross’, respectively. Following ‘sequence’, digits 1–5 were sequentially displayed for 300 ms at a frequency of 1 digit/s. Presentation of the numerical sequence was followed by a delay (~6 s) during which subjects had to prepare for the next task to perform, knowing that digits 1, 2, 3, 4, and 5 referred to the thumb, index, middle, ring, and little fingers of the right hand, respectively. Participants did not know the sequences in advance, and different numerical sequences were used for each cycle. Twelve seconds after onset of the first condition, ‘movement’ was displayed on the screen, cueing subjects to recall and reproduce the numerical sequence four times in a row from memory by pressing on response keys using brisk finger movements (20 finger movements in total). Each finger movement was visually triggered by a cross displayed on the screen for 300 ms at unpredictable intervals with an average frequency of ~0.5 Hz. No feedback was given to the subjects regarding their accuracy. Finally, the baseline block (‘fixation cross’) in each cycle started 48 s after the ‘movement’ block onset. The block consisted of presenting visual stimuli identical to those used in the movement block but no movement was required. Emphasis was placed on watching the fixation point on the center of the screen where a cross was displayed 20 times for 300 ms at unpredictable intervals with a average frequency of ~0.5 Hz. Prior to scanning, all participants were allowed to practice the task paradigm for 10 min outside and then inside the magnet.

Visual stimuli were generated and subject responses recorded by a personal computer using COGENT Cognitive interface software (COGENT 2000, Wellcome Department of Imaging Neuroscience, London, UK) implemented in Matlab 5.3 (Mathworks, Sherborn, MA). Behavioral data were subsequently analyzed using Matlab. From the task, accuracy and response time (RT) were computed as indices of motor performance. If subjects pressed the wrong key or if RT was longer then 1300 ms, the computer program registered an error and this key press was excluded from the RT data analysis.

fMRI data acquisition

Imaging was performed on a whole-body 3.0-T GE Signa system (GE medical systems, Milwaukee, WI) equipped with gradients capable of 40 mT/m amplitude and 150 T/m/s slew rate. The hardware used to obtain ASL data was identical to that described in Talagala et al. (2004a). In brief, separate coils were used for labeling and imaging. A custom-made surface coil designed as two rectangular loops (6.6 cm × 4.5 cm) was placed on the neck of the subject to label blood flowing in the right and left carotid and vertebral arteries. The labeling coil, tuned to 127.8 MHz, was connected to an external RF channel controlled by the scanner. The frequency of RF applied to the labeling coil was offset 16–20 kHz from center frequency according to the distance from the isocenter to the labeling coil and the gradient strength during the labeling period. Imaging was performed using a detunable, 27-cm diameter, volume transmit/receive coil (Nova Medical, Inc. Wakefield, MA). During the labeling period, the labeling coil was tuned and the volume coil was detuned. The tuning status of the coils was reversed at all other times.

The time series began with dummy gradients and RF pulses corresponding to the first four images to allow brain tissue to reach steady state magnetization. Then, temporally interleaved multislice images without (even images) and with (odd images) labeling were collected every 6 s (effective TR) for 10 min 48 s. Control and arterial spin-labeled images were obtained by reversing the polarity of the gradient applied during the labeling period while the frequency of the RF applied to the labeling coil was held fixed. The 6-s interval included three periods. First, RF power (1.7 W) was applied to the labeling coil for 4 s in the presence of a 0.3 G/cm gradient along the superior/inferior direction. Second, after labeling, a delay of 1200 ms was introduced before image acquisition in order to reduce the signal from larger vessels and to reduce the perfusion signal dependence on blood transit time between the labeling and imaging zones (Alsop and Detre, 1996; Gonzalez-At et al., 2000). Third, at the end of the postlabeling delay, 13 axial slices were acquired sequentially from superior to inferior in 800 ms using a single-shot 2D gradient-echo echo-planar imaging (GRE-EPI) sequence (slice thickness = 5 mm, slice gap = 3 mm, TE = 13 ms, flip angle = 90°; bandwidth 62.5 kHz; matrix size 64 × 64, yielding an in-plane resolution of 3.75 mm × 3.75 mm). The axial extent of the data set was 101 mm, which allowed coverage from the top of the brain to the top of the cerebellum. A relatively larger slice gap was used to minimize signal distortion due to interslice cross-talk. The sequential acquisition of slices every 61.5 ms means that the postlabeling delay was not identical for each slice, increasing from superior to inferior. There were two behaviorally identical fMRI sessions, allowing acquisition of 108 pairs of control and arterial spin-labeled images for each participant.

Image processing

Offline data processing and analysis were performed on a Linux workstation using the Statistical Parametric Mapping Software (SPM2, Wellcome Department of Imaging Neuroscience, London, UK; freely available at http://www.fil.ion.ucl.ac.uk/spm) implemented within Matlab 6. All images were initially checked for gross artifacts and manually reoriented to grossly conform to the orientation of the interhemispheric fissure and intercommissural plane of the canonical EPI template image proposed as default in SPM2. The center point was placed approximately on the anterior commissure. Images within each time series were realigned to the first acquisition using rigid-body transformations and the most accurate function for realignment in SPM2.

After realignment, session-specific time series of perfusion data were generated as follows. Fractional signal change images ($\Delta S/S_c$*100) were computed from each pair of control and labeled images, where ΔS is the pairwise magnitude difference in signal between temporally adjacent control and labeled images and S_c is the signal of the control image. Using fractional signal change images allows CBF changes to be measured without contamination from BOLD signal changes. In order to remove abnormal flow values, a double intensity threshold was included in the procedure to retain only (1) pairs of voxels whose control signal intensity had a value greater than 80% of the global mean intensity of the control image, and (2) voxels in the fractional signal change image with intensity within the range ±5%. We will refer to these 'thresholded $\Delta S/S_c$ images' as perfusion-weighted images. Some raw images (<2% of all raw data) were severely corrupted with high-intensity artifacts across the field-of-view due to malfunctioning of the labeling amplifier blanking electronics during image acquisition. Thus, corresponding perfusion-weighted images could not be created. Under those circumstances, the missing perfusion-weighted image in the time series was reconstructed by averaging the two temporally adjacent perfusion-weighted images.

All perfusion-weighted images were subsequently processed to examine results at the population level. The first EPI image of each time series was spatially normalized to the standard EPI template proposed as default in SPM2. This SPM template is in MNI space (Montreal Neurological Institute, http://www.bic.mni.mcgill.ca) and approximates the standard stereotaxic space of Talairach and Tournoux (1988). Linear and nonlinear deformation parameters estimated during this step were then subsequently applied to the corresponding perfusion-weighted time series generated in the preceding step. Spatially normalized images were resliced to a voxel size of 3 × 3 × 3 mm and smoothed using an 8-mm FWHM Gaussian kernel.

Image analysis

Absolute resting state CBF quantification

The resting state gray matter CBF within a cortical region-of-interest (ROI) was calculated using the $\Delta S/S_c$ signal averaged across the time series in native space using the following equation derived from Talagala et al. (2004a):

$$\mathrm{CBF} = \frac{\Delta S}{S_c} \; \frac{\lambda}{2\alpha e^{-\delta(R_{1a}-R_{1obs})}} \; \frac{R_{1obs}}{e^{-R_{1obs}w}} \; \frac{(1-e^{-R_{1obs}\mathrm{TR}})}{(1-e^{-R_{1obs}\tau})} \qquad (1)$$

where, R_{1obs} is the T_1 relaxation rate of gray matter, R_{1a} is the T_1 relaxation rate of arterial blood, α is the labeling efficiency at the

labeling site, w is the postlabeling delay, δ is the arterial blood transit time from the labeling site to tissue, τ is the labeling duration, λ is the brain–blood partition coefficient, and TR is the effective repetition time. For CBF quantification, a value of 0.75 was used for α (Talagala et al., 2004a) for all subjects and δ was assumed to be 1 s (Butman et al., 2002). λ was assumed to be 0.9 ml/g (Herscovitch and Raichle, 1985), $R_{1a} = 0.67\ s^{-1}$, $R_{1obs} = 0.75\ s^{-1}$, τ = 4 s, TR = 6 s, and w was 1.20–1.94 s depending on the slice. CBF quantitation was performed using ROI measurements taken from the rostral part of the left frontal cortex, a region that showed no significant variation of flow between baseline and the motor task (vide infra).

Statistical parametric mapping

Realigned, spatially normalized, and smoothed perfusion-weighted time series were analyzed using SPM2 in the framework of the general linear model (GLM) (Friston et al., 1995). A first-level analysis was initially performed to accommodate for within-subject, between-scan variability. Since our goal was to examine task-related changes in perfusion signal in our population taken as a group, a second level–level analysis was then carried out to take into account possible subject-by-condition interactions, as previously proposed (Holmes and Friston, 1998).

In within-subject (first-level) analyses, data acquired during the two behaviorally identical fMRI sessions were included in a single, subject-specific, design matrix. We used statistical models for PET data ('The Full Monty') in SPM2 with the assumption of the absence of temporal autocorrelation of the data under the null hypothesis. Evidence to date suggests that this assumption is valid for perfusion data acquired with ASL-based fMRI techniques (Aguirre et al., 2002; Wang et al., 2003b). In addition to the six regressors of interest modeling each of the three experimental conditions for both fMRI sessions, the statistical model included two additional regressors representing each fMRI session as a block effect. Finally, the global mean intensity of each image was also incorporated as a regressor in the design matrix (ANCOVA) (Friston et al., 1990). It has been proposed that this approach might account for fluctuations in signal intensity due to physiological noise and might improve the central tendency of the distribution of test statistic when analyzing ASL-based fMRI data (Wang et al., 2003b). Rather than including voxels that have intensities higher than 80% of the global brain mean (which is done by default in SPM), we explicitly specified which voxels to be included in the statistical analysis by using subject-specific binary mask images derived from raw fMRI data. Parameter estimates and variance were derived voxel-by-voxel for each regressor. Voxels showing statistically significant task-related changes in blood flow were identified using a two-tailed contrast testing for an increase or a decrease in intensity during the movement condition compared to the visual control condition (baseline).

In the context of a random-effect model, in which a single measurement is obtained from each subject (Friston et al., 1999; Holmes and Friston, 1998), individual contrast images from level 1 analyses were entered in a second-level one-sample t test to create an SPM{t} (14 degrees of freedom). This analysis appropriately accounts for intersubject variability and tests whether or not the population from which our set of subjects is drawn possesses the hypothesized effect. Group results were characterized in terms of the probability that the variation in magnitude value in a given voxel could occur by chance under the null hypothesis. In the analysis testing for a relative increase in flow during finger movements, the significance level was set at a P value < 0.05 after correction for multiple comparisons using the false discovery rate (FDR) (Genovese et al., 2002) as implemented in SPM2. In the analysis testing for a negative perfusion response, the correction was limited to a spherical volume (small volume correction, SVC) around regions where this effect was hypothesized, namely in ipsilateral S1M1 and medial parietal areas. The radius of the spherical volume was defined at 5 mm. This approach is commonly accepted in the neuroimaging community (Thieben et al., 2002). A cluster size threshold of 15 voxels in any direction was always applied as an additional procedure for removing false-positive foci from the SPM{t} (Forman et al., 1995).

Anatomical localization was performed by superimposing the maxima of activation and deactivation foci identified by the second level analysis SPM{t} on the mean spatially normalized perfusion images from all study subjects. This approach takes into account the variance of brain structures between subjects under investigation and spatial distortions inherent to EPI images. Anatomical labeling was performed with the aid of the atlas of Duvernoy et al. (1999) and by reference to human probabilistic atlases (Geyer et al., 1996) when appropriate. This approach has obvious limitations and the designation of the anatomic structures is tentative rather than definitive.

Percent rCBF changes

Percent rCBF changes in regions showing a significant result in the second-level analysis were estimated from a first-level group (between-subjects) analysis including spatially normalized and smoothed perfusion-weighted images from all session study subjects. For each subject and session, regional increases and decreases in blood flow specific to the contrasts of interest were estimated from beta images using the MarsBar region of interest (ROI) toolbox for SPM (freely available at http://marsbar.sourceforge.net/) (Brett et al., 2002).

Results

Task performance

Twenty-nine of thirty session-specific data sets were incorporated in the behavioral data analysis. Data from one fMRI session could not be saved on the PC. The mean accuracy across subjects was 95%. Among the 5% of errors, 60% were incorrect responses and 40% were omitted key presses. The group average RT (mean ± standard deviation) was 394 ± 83 ms (range 293–620 ms).

Imaging data

Fig. 1 shows 12 of 13 slices of a perfusion-weighted image set in native space from a representative subject. Perfusion in all brain regions, including the cerebellum, is visualized with good sensitivity. This indicates that a high labeling efficiency was achieved in the carotid and vertebral arteries on both sides of the neck. Reduced intensity in the lowest slices is because these slices corresponded to the longest postlabeling delays. The fractional signal change $\Delta S/S_c$*100 (mean ± standard deviation) due to labeling averaged across subjects within a cortical ROI in the left frontal cortex was 0.78 ± 0.18%. This corresponds to a CBF value (mean ± standard deviation) of 63 ± 15 ml 100 g^{-1} min^{-1}.

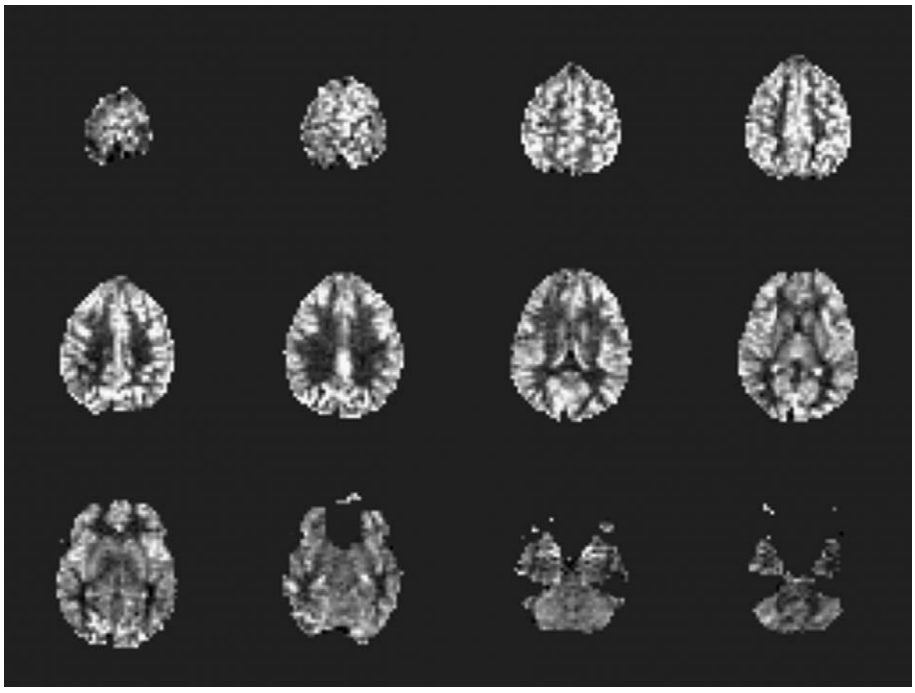

Fig. 1. Perfusion-weighted image in native space from a representative subject (total acquisition time: 8 min, 20 s). Slices were acquired sequentially from top to bottom. Only the last 12 slices (out of 13) are shown. Note the decrease in perfusion signal intensity from the upper to the lower slice.

Relative increase in rCBF during movements

Table 1 summarizes the center of mass in MNI space and Z values in the second level analysis ($P < 0.05$, FDR corrected). For each peak, the estimated average rCBF change normalized to baseline flow is also given. The largest increase in rCBF was detected in the HRA of the left primary motor cortex (M1) (mean ± standard deviation = 31 ± 17%) (Fig. 2) (Yousry et al., 1997). Other cortical activations included dorsal lateral premotor cortices and intraparietal sulci bilaterally, left ventral lateral premotor cortex, supplementary motor area proper (SMA proper), middorsal lateral prefrontal cortex (DLPFC), inferior and superior parietal cortices, insular cortex, parietal operculum (second somatosensory cortex), and medial parietal areas including precuneus. At the subcortical level, increased flow was found in the HRA of the left putamen (Maillard et al., 2000), ventrolateral and centromedian thalamic nuclei, and the anterior part of the right superior cerebellar hemisphere.

Relative decrease in rCBF during movements

According to our a priori hypothesis, our analysis focused on medial parietal areas and ipsilateral S1M1. We report a decrease in perfusion signal during movements compared to baseline in the right posterior cingulate sulcus. There was also a negative perfusion response (NPR) in the HRA of M1 ipsilateral to the movements (Table 2, Fig. 3). A trend toward significance was observed in the left posterior cingulate sulcus ($P = 0.051$, SVC) as well as in the upper part of the HRA of M1 ipsilateral to the movements ($P = 0.055$, SVC). Inspection of individual maps showed that there was a substantial interindividual variability in the topography and magnitude of the NPR along the central sulcus. The flow change (mean ± standard deviation) in the right M1 averaged across subjects was −6 ± 12% (ranging from −29% to +25%).

Discussion

Noninvasive measurement of task-associated changes in rCBF using ASL-based fMRI emerges as an attractive alternative to BOLD fMRI. However, existing multislice ASL fMRI techniques are limited by several factors. One of these is the extent of the imaging region: ASL imaging of lower brain regions and cerebellum is generally accompanied by reduced labeling efficiency and SNR. In this context, our results demonstrate that multislice CASL fMRI using a two-coil system can be used to map task-related changes in rCBF in cortical areas, striatum, thalamus, and cerebellar brain regions.

To test our method, imaging data were acquired during a blocked design experimental paradigm in which performance of visually triggered memory-guided motor sequences alternated with a passive visual stimulation (baseline). The differences in blood flow between these conditions should identify brain areas involved in motor sequence control. As predicted by a large number of functional brain mapping studies, increased flow was indeed detected in a 'motor sequence execution' network. The largest increase in rCBF was found in the HRA (Yousry et al., 1997) of left M1 (contralateral to the moving hand). Furthermore, significant increase in rCBF was detected in other key components of this network including the rostral part of left SMA proper, the caudal part of the left anterior cingulate sulcus adjacent to SMA [caudal cingulate zone, CCZ (Picard and Strick, 2001)], the HRA of the left posterior putamen (Maillard et al., 2000), left ventrolateral thalamus, and the anterior part of the right cerebellar hemisphere (Catalan et al., 1998; Colebatch et al., 1991; Haslinger et al., 2002; Sadato et al., 1996). It should be emphasized that despite the reduced perfusion signal in slices acquired later (i.e., covering the bottom half of the brain and cerebellum; Fig. 1) resulting in a smaller statistical power for these slices (vide supra Introduction), SNR was still sufficient to detect significant changes in rCBF

Table 1
Main areas showing a relative increase in CBF during memory-guided, visually triggered sequential finger movements compared to baseline (second-level analysis)

	Coordinates[a]			Z value	Percent rCBF increase[b]
	x	y	z		
Cortical areas					
Left hemisphere					
Precentral gyrus (HRA), M1	−39	−24	57	5.71	31 ± 17
Superior frontal sulcus (post. part), PMd	−24	−9	51	5.20	19 ± 13
Postcentral gyrus, S1	−51	−21	54	4.93	27 ± 18
	−54	−27	48	4.83	21 ± 12
Middle frontal gyrus, PMd	−33	6	57	4.81	9 ± 9
Anterior cingulate sulcus, CCZ	−3	0	48	4.78	11 ± 7
Intraparietal sulcus (ant. part)	−45	−36	45	4.69	18 ± 11
	−45	−24	27	4.23	16 ± 15
Superior frontal gyrus, PMd	−12	−9	69	4.38	9 ± 9
Inferior frontal gyrus (pars opercularis), PMv	−57	6	18	4.64	13 ± 11
Superior temporal sulcus (asc. post. segment)	−51	−45	24	4.46	11 ± 12
Superior parietal lobule	−21	−69	57	4.34	23 ± 26
Medial frontal gyrus, SMA proper	−3	−6	57	4.19	13 ± 9
Parietal operculum, SII	−48	−21	18	4.03	11 ± 18
Insular cortex	−45	6	6	4.03	8 ± 12
Posterior cingulate cortex	−3	−24	27	4.01	8 ± 8
Precuneus	−9	−75	42	3.87	10 ± 10
Inferior parietal lobule	−54	−42	51	3.79	9 ± 10
Middle frontal gyrus, DLPFC	−39	45	30	3.39	9 ± 14
	−36	33	27	3.24	10 ± 13
Anterior cingulate gyrus	−6	15	30	3.34	6 ± 8
Right hemisphere					
Intraparietal sulcus (middle part)	33	−42	33	3.75	16 ± 25
	42	−45	42	3.13	10 ± 14
Anterior cingulate gyrus	15	18	45	3.50	9 ± 13
Superior frontal sulcus (post. part), PMd	39	−6	60	3.50	8 ± 10
Postcentral gyrus, S1	51	−27	45	2.99	8 ± 11
Subcortical areas					
Left thalamus centromedian	−12	−21	3	4.26	11 ± 10
Left thalamus ventrolateral	−9	−12	3	3.54	12 ± 13
Right cerebellum (quadrangular lobule)	24	−54	−27	3.49	17 ± 34
Left putamen (HRA)	−27	3	3	3.33	6 ± 11

[a] Coordinates (in millimeters) of peaks in MNI space are given for information. Anatomic localization was performed with the aid of the atlas of Duvernoy (see Methods).
[b] Mean ± standard deviation (N = 15). M1 = primary motor cortex, HRA = hand representation area, PMd = dorsal lateral premotor cortex, S1= primary sensory cortex, CCZ = caudal cingulate zone, PMv = ventral lateral premotor cortex, SMA = supplementary motor area, SII = secondary sensory area, DLPFC = dorsal lateral prefrontal cortex, ant. = anterior, post. = posterior.

across subjects in left putamen and thalamus and right cerebellum (Table 1, Fig. 2).

Our behavioral paradigm also involved participation of more elaborate processes than those related to the execution of sequential movements. First, different delayed, visually presented sequences were used for each movement epoch in a way similar to the spatial span of Corsi (see Milner, 1971), a task that is commonly used to assess working memory performance. Second, since there was a visual input and a motor output, the task required visuomotor mapping processes. Third, individual finger movements were triggered by visual cues presented at unpredictable intervals. An accurate and quick response as shown by the behavioral results therefore required a significant degree of visual and sensory (i.e., kinesthetic) monitoring and individual finger movement preparation. It was not the goal of our experiment to disentangle the neural substrate underlying all those processes. However, increased flow in the left dorsolateral prefrontal area as well as bilateral premotor-parietal networks predominant on the left including intraparietal sulci and the posterior part of superior temporal sulcus as illustrated in Fig. 2 is consistent with results from previous studies on high order aspects of motor control (Deiber et al., 1996; Grafton et al., 1995; Menon et al., 2000; Sadato et al., 1996; Sakai et al., 1998; Toni et al., 2002). The absence of activation in pre-SMA, a region located on the medial wall of cerebral hemispheres rostral to the coronal plane through the anterior commissure, agrees well with results from the BOLD fMRI study of Thickbroom et al. (2000), who found only a weak activation in pre-SMA compared to SMA-proper during visually triggered movements, even when movement timing was not predictable as in the present study. Hence, the absence of detected activation in pre-SMA might be more related to the nature of the experimental design we used rather than a lack of sensitivity of our method.

In accordance with our a priori hypothesis, a relative decrease in flow was detected in medial parietal areas and the HRA of M1 ipsilateral to the moving hand (Table 2). Decreased activity in the medial parietal areas during active tasks compared to baseline is a

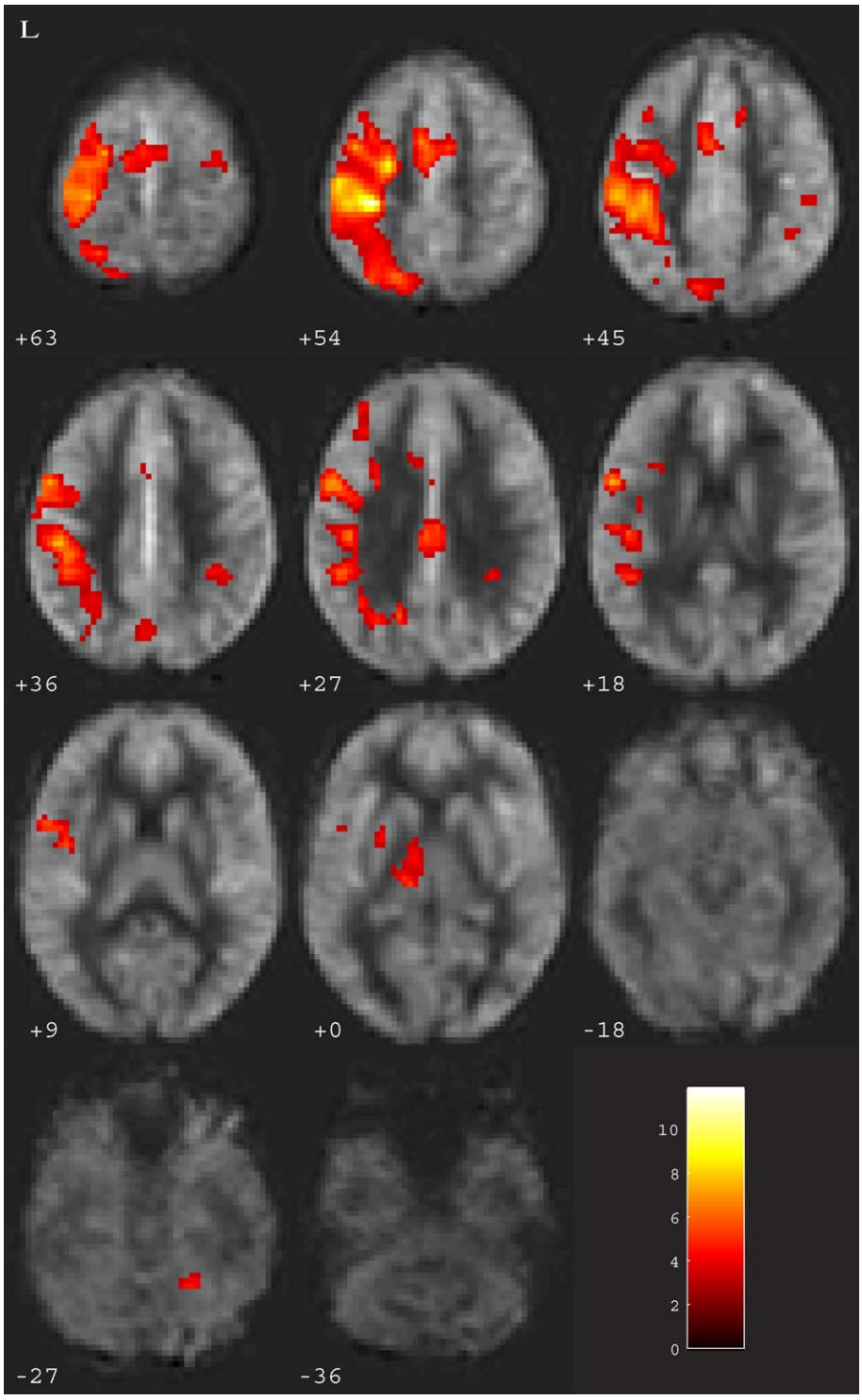

Fig. 2. Brain areas showing increased flow during unimanual (right hand) finger movements compared to baseline ($P < 0.05$ FDR corrected). Group results are superimposed on 11 axial slices through the mean perfusion-weighted image in standard stereotaxic space from all 15 study subjects. The pseudocolor scale corresponds to the T values from the random effect analysis. Values in the lower left corner of each image indicate the distance (in mm) of the image from the axial plane through the anterior and posterior commissures. Results are presented in neurological convention. Note the detection of a significant increase in rCBF in subcortical structures including the left putamen, thalamus, and the superior and anterior part of the right cerebellar hemisphere.

reproducible finding in the functional imaging literature and its significance has recently been discussed by Raichle et al. (2001). The presence of a sustained negative BOLD response (NBR) in the HRA of ipsilateral M1 has been reported by several authors in healthy subjects during movements of ipsilateral fingers or hand compared with baseline (Allison et al., 2000; Hsieh et al., 2002; Reddy et al., 2000). Our group results provide some evidence to suggest that this NBR, which can be modeled as a complex interplay between relative CBF, cerebral blood volume (CBV), and oxygen extraction (Shmuel et al., 2002), is accompanied by a negative

Table 2
Main areas showing a relative decrease in rCBF during the task compared to baseline

	Coordinates			Z value	Percent rCBF decrease
	x	y	z		
Right hemisphere					
Precentral gyrus, M1 (area 4 p)	36	−21	45	2.35	−6 ± 12
*	24	−24	63	2.33	−6 ± 13
Posterior cingulate sulcus	9	−27	45	3.86	−4 ± 6
Left hemisphere					
*Posterior cingulate sulcus	−12	−42	45	2.28	−3 ± 9

The legend of the table is similar to that of Table 1. Brain regions marked with an * shows trend toward significance (see Results).

perfusion response (NPR). Geyer et al. (1996) demonstrated that there were at least two anatomically and functionally distinct representations of fingers in M1 Brodmann's area 4: subareas 4a and 4p. Projection of results on the population-averaged perfusion-weighted image showed that the peak NPR found in the present study is preferentially located in an area encompassing M1 subarea 4p (Fig. 3) (Binkofski et al., 2002). This peak could be distinguished from a positive perfusion response (PPR) located in a more lateral and caudal region most likely corresponding to ipsilateral S1. Analysis of individual deactivation maps showed that there was a substantial interindividual variability in the topography and magnitude of the NPR along the central sulcus (data not shown). This may explain why this NPR is difficult to detect from second-level analyses. Variability of deactivation in ipsilateral M1 seems to be a consistent finding in existing fMRI studies (Allison et al., 2000; Hamzei et al., 2002; Reddy et al., 2000). Little is known either about the source of this interindividual variability or on the mechanisms underlying this negative response. Results from Binkofski et al. (2002) suggest that activity in M1 area 4p might be modulated by attention to action, whereas activity in area 4a might not. Based on that report, we speculate that the observed NPR in area 4p might have a neuronal origin arising from decreased attention to the contralateral hand during ipsilateral hand movements. Alternatively, several authors have argued that transcallosal inhibition from the contralateral M1 hand area may play a role in deactivation in ipsilateral M1 (Allison et al., 2000; Hamzei et al., 2002), although this hypothesis has been questioned by an fMRI study conducted in acallosal patients (Reddy et al., 2000). Clearly, more work is needed to clarify these issues.

Altogether, the spatial distribution of relative cortical and subcortical blood flow increases and decreases is fairly consistent with results from previous functional imaging studies suggesting that CASL fMRI using a separate labeling coil provides adequate sensitivity and accuracy to map task-related changes in CBF in the cortex, basal ganglia, and cerebellar areas.

In addition to their topography, task-induced changes in rCBF could also be characterized by their magnitude relative to baseline (Tables 1 and 2). Quantification of resting state gray matter CBF provides an average value of 63 ml 100 g^{-1} min^{-1} in a cortical ROI. This is roughly similar to the resting flow values in gray matter previously reported in healthy subjects using CASL MRI (Ye et al., 2000) and PET (Frackowiak et al., 1980). Compared to baseline, M1 contralateral to the moving fingers showed an average 31% increase in flow during movements. This is significantly lower than the 70–130% increases in rCBF reported by most ASL fMRI studies (Buxton et al., 1998; Mildner et al., 2003; Ye et al., 1997; Yongbi et al., 2002). This apparent discrepancy may have a physiological basis. Indeed, based on the well-described positive relationship between movement frequency and magnitude changes in brain activity (Sadato et al., 1997), participants in previous ASL fMRI studies were generally asked to execute finger movements at a frequency of 1 Hz or higher in order to maximize peak activation in contralateral M1 cortex. In contrast to those studies, slightly more than 2 s elapsed on average between individual finger movements in the present study. Thus, the smaller flow increase

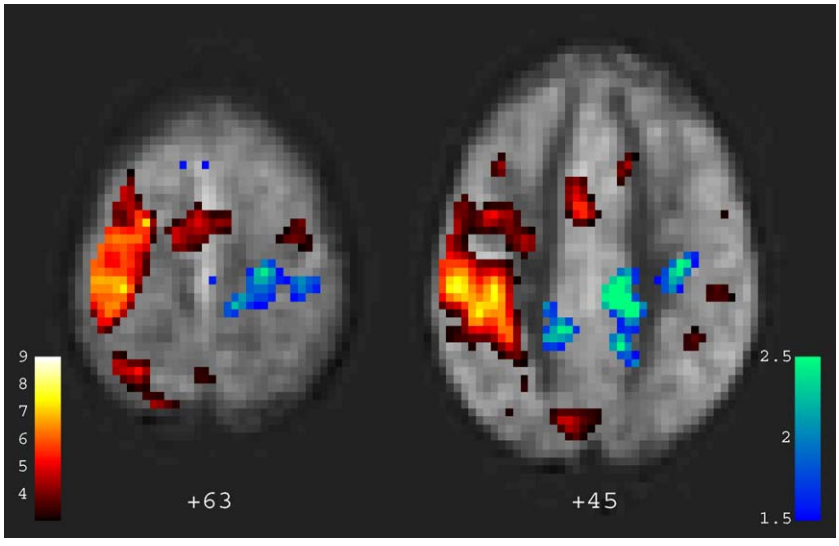

Fig. 3. Decreased flow (in blue–green) in medial parietal areas and ipsilateral M1 during unimanual finger movements (random effect analysis). Areas showing increased CBF (in red–yellow) in the same slices are given for comparison. The decrease in CBF in ipsilateral M1 is preferentially located in the deep portion of area 4 presumably area 4p (Geyer et al., 1996). On the right-sided image (+45), this peak could be distinguished from an area of increased CBF located in a slightly more lateral and caudal area most likely corresponding to ipsilateral S1. The pseudocolor scales correspond to *T* values from the random effect analysis. Other image conventions are identical to those described in Fig. 2.

found here in contralateral M1 compared with previous ASL-based fMRI studies is consistent with the known physiology of M1.

A comparison with magnitude changes reported in previous PET studies during similar task paradigms requires caution (Zaini et al., 1999). The reconstructed images in the most recent CBF PET studies on the motor system had a in-plane resolution of about 7 × 7 mm (Deiber et al., 1996; Jenkins et al., 2000) whereas the in-plane resolution of our raw images was 3.75 × 3.75 mm. This difference in spatial resolution is further magnified by spatially convolving the data with a Gaussian kernel, which is usually larger in PET than for fMRI data. Yet, it has been shown that percent flow changes can vary as a function of image smoothness: the higher the smoothness, the lower the magnitude change (Ye et al., 1997). This obviously makes quantitative comparisons of results difficult to interpret across independent PET and fMRI studies, and indeed, magnitude changes reported here are generally higher than those measured in previous PET studies (Deiber et al., 1996; Jenkins et al., 2000).

The main limitation of the present method is a relatively poor temporal resolution. Temporal resolution could be improved by optimizing the duration of labeling. Preliminary experiments in our laboratory indicate that SNR per unit acquisition time and temporal resolution can be increased by using a labeling period of ~2.5 s instead of 4 s (Chuang et al., 2004). Moreover, new acquisition schemes are being developed to permit collection of multislice subtraction pairs in less than 3 s using CASL fMRI and a two-coil system but they are not directly applicable to whole brain fMRI studies yet (Hernandez-Garcia et al., 2004). A higher SNR in the present method can be achieved by using multiple channel receiver coil arrays. When combined with parallel imaging techniques, the SNR gained can be used to increase the number of slices imaged, improve resolution, or reduce scan time (Talagala et al., 2004b).

In this study, the perfusion time series were generated by calculating the fractional signal change between the temporally adjacent control and label images. This approach suppresses the BOLD contribution to the measured task-related CBF change if pairs of control and label image have the same BOLD weighting. However, when using short TR, the pairs of control and label images acquired near the beginning and end of each block may have different BOLD weighting because of finite time (~6 s) required for the BOLD effect to reach a steady state. It has been shown that this error can be minimized by using sinc interpolation to create time-matched control and label images (Aguirre et al., 2002). In the experimental protocol used here, the first control ASL image in each movement and baseline condition was acquired 5.2–5.9 s after the start of the block when the BOLD effect has almost reached the steady state. Therefore, any error due to differential BOLD weighting in adjacent control and label images is expected to be small.

We have shown that perfusion-based fMRI using 2D CASL imaging with a separate labeling coil provides sufficient SNR to map, at the population level, task-related flow changes in cortical, basal ganglia, and cerebellar areas with adequate accuracy and sensitivity in a blocked-design experiment. Although brain imaging relying on BOLD contrast remains the technique of choice for most fMRI applications, the present study represents an important step toward an increased use of ASL fMRI in humans.

Acknowledgments

GG is a postdoctoral researcher at the ‘Fonds National de la Recherche Scientifique Belge’ (FNRS). GG is also supported by grants from the ‘Fondation Horlait-Dapsens’, the Belgian American Educational Foundation (BAEF), NATO, and NINDS. The authors would like to thank Alan Koretsky, PhD, for many stimulating discussions on applications of ASL techniques, Wen-Ming Luh, PhD, and Peter Bandettini, PhD, for discussions on data analysis; Nguyet Dang for technical assistance; Paula Rowser for help in image acquisition; and Devera Schoenberg, MSc, for skillful manuscript editing.

References

Aguirre, G.K., Detre, J.A., Zarahn, E., Alsop, D.C., 2002. Experimental design and the relative sensitivity of BOLD and perfusion fMRI. NeuroImage 15, 488–500.

Allison, J.D., Meador, K.J., Loring, D.W., Figuaroa, R.E., Wright, J.C., 2000. Functional MRI cerebral activation and deactivation during finger movement. Neurology 54, 135–142.

Alsop, D.C., Detre, J.A., 1996. Reduced transit-time sensitivity in noninvasive magnetic resonance imaging of human cerebral blood flow. J. Cereb. Blood Flow Metab. 16, 1236–1249.

Barbier, E.L., Lamalle, L., Decorps, M., 2001. Methodology of brain perfusion imaging. J. Magn. Reson. Imaging 13, 496–520.

Binkofski, F., Fink, G.R., Geyer, S., Buccino, G., Gruber, O., Shah, N.J., Taylor, J.G., Seitz, R.J., Zilles, K., Freund, H.J., 2002. Neural activity in human primary motor cortex areas 4a and 4p is modulated differentially by attention to action. J. Neurophysiol. 88, 514–519.

Brett, M., Anton, J.L., Valabregue, R., Poline, J.B., 2002. Region of interest analysis using an SPM toolbox. Presented at the 8th International Conference on Functional Mapping of the Human Brain, Sendai, Japan. Available on CD-ROM in NeuroImage, Vol. 16, no. 2, abstract 497.

Butman, J.A., Rebmann, A.J., Talagala, S.L., 2002. Abstract. Measurement of regional cervical–cerebral arterial transit time at high temporal resolution using dynamic susceptibility contrast. In: Proceedings of the 10th Annual Meeting of ISMRM, Honolulu, HI, USA, p. 1076.

Buxton, R.B., Frank, L.R., Wong, E.C., Siewert, B., Warach, S., Edelman, R.R., 1998. A general kinetic model for quantitative perfusion imaging with arterial spin labeling. Magn. Reson. Med. 40, 383–396.

Catalan, M.J., Honda, M., Weeks, R.A., Cohen, L.G., Hallett, M., 1998. The functional neuroanatomy of simple and complex sequential finger movements: a PET study. Brain 121, 253–264.

Chuang, K.-H., Chesnick, S., Koretsky, A.P., Talagala, S.L., 2004. Abstract. Optimization of the labeling time for continuous arterial spin labeling MRI. Proc. ISMRM 11, 1364.

Colebatch, J.G., Deiber, M.-P., Passingham, R.E., Friston, K.J., Frackowiak, R.S.J., 1991. Regional cerebral blood flow during voluntary arm and hand movements. J. Neurophysiol. 65, 1392–1401.

Deiber, M.-P., Ibanez, V., Sadato, N., Hallett, M., 1996. Cerebral structures participating in motor preparation in humans: a positron emission tomography study. J. Neurophysiol. 75, 233–247.

Detre, J.A., Leigh, J.S., Williams, D.S., Koretsky, A.P., 1992. Perfusion imaging. Magn. Reson. Med. 23, 37–45.

Duong, T.Q., Kim, D.S., Ugurbil, K., Kim, S.G., 2001. Localized cerebral blood flow response at submillimeter columnar resolution. Proc. Natl. Acad. Sci. U. S. A. 98, 10904–10909.

Duvernoy, H.M., 1999. The human brain. Surface, Blood Supply, and Three Dimensional Sectional Anatomy, second ed. Springer-Verlag, Wien New York.

Edelman, R.R., Siewert, B., Darby, D.G., Thangaraj, V., Nobre, A.C., Mesulam, M.M., Warach, S., 1994. Qualitative mapping of cerebral blood flow and functional localization with echo-planar MR imaging and signal targeting with alternating radio frequency. Radiology 192, 513–520.

Forman, S.D., Cohen, J.D., Fitzgerald, M., Eddy, W.F., Mintun, M.A., Noll, D.C., 1995. Improved assessment of significant activation in functional

magnetic resonance imaging (fMRI): use of a cluster-size threshold. Magn. Reson.Med. 33, 636–647.
Frackowiak, R.S., Lenzi, G.L., Jones, T., Heather, J.D., 1980. Quantitative measurement of regional cerebral blood flow and oxygen metabolism in man using 15O and positron emission tomography: theory, procedure, and normal values. J. Comput. Assist. Tomogr. 4, 727–736.
Friston, K.J., Frith, C.D., Liddle, P.F., Dolan, R.J., Lammerstma, A.A., Frackowiak, R.S.J., 1990. The relationship between global and local changes in PET scans. J. Cereb. Blood Flow Metab. 10, 458–466.
Friston, K.J., Holmes, A.P., Worsley, K.J., Poline, J.B., Frith, C.D., Frackowiak, R.S.J., 1995. Statistical parametric maps in functional imaging: a general linear approach. Hum. Brain Mapp. 2, 189–210.
Friston, K.J., Holmes, A.P., Price, C.J., Buchel, C., Worsley, K.J., 1999. Multisubject fMRI studies and conjunction analyses. NeuroImage 10, 385–396.
Genovese, C.R., Lazar, N.A., Nichols, T., 2002. Thresholding of statistical maps in functional neuroimaging using the false discovery rate. NeuroImage 15, 870–878.
Geyer, S., Ledberg, A., Schleicher, A., Kinomura, S., Schormann, T., Burgel, U., Klingberg, T., Larsson, J., Zilles, K., Roland, P.E., 1996. Two different areas within the primary motor cortex of man. Nature 382, 805–807.
Gonzalez-At, J.B., Alsop, D.C., Detre, J.A., 2000. Cerebral perfusion and arterial transit time changes during task activation determined with continuous arterial spin labeling. Magn. Reson. Med. 43, 739–746.
Grafton, S.T., Hazeltine, E., Ivry, R., 1995. Functional mapping of sequence learning in normal humans. J. Cogn. Neurosci. 7, 497–510.
Hamzei, F., Dettmers, C., Rzanny, R., Liepert, J., Buchel, C., Weiller, C., 2002. Reduction of excitability ("inhibition") in the ipsilateral primary motor cortex is mirrored by fMRI signal decreases. NeuroImage 17, 490–496.
Haslinger, B., Erhard, P., Weilke, F., Ceballos-Baumann, A.O., Bartenstein, P., Grafin, v.E., Schwaiger, M., Conrad, B., Boecker, H., 2002. The role of lateral premotor–cerebellar–parietal circuits in motor sequence control: a parametric fMRI study. Brain Res. Cogn. Brain Res. 13, 159–168.
Hernandez-Garcia, L., Lee, G.R., Vazquez, A.L., Noll, D.C., 2004. Fast, pseudo-continuous arterial spin labeling for functional imaging using a two-coil system. Magn. Reson. Med. 51, 577–585.
Herscovitch, P., Raichle, M.E., 1985. What is the correct value for the brain–blood partition coefficient for water. J. Cereb. Blood Flow Metab. 5, 65–69.
Holmes, A.P., Friston, K.J., 1998. Generalisability, random effects, and population inference. NeuroImage 7, 754.
Hsieh, J.C., Cheng, H., Hsieh, H.M., Liao, K.K., Wu, Y.T., Yeh, T.C., Ho, L.T., 2002. Loss of interhemispheric inhibition on the ipsilateral primary sensorimotor cortex in patients with brachial plexus injury: fMRI study. Ann. Neurol. 51, 381–385.
Jenkins, I.H., Jahanshahi, M., Jueptner, M., Passingham, R.E., Brooks, D.J., 2000. Self-initiated versus externally triggered movements: II. The effects of movement predictability on regional cerebral blood flow. Brain 123, 1216–1228.
Kim, S.G., 1995. Quantification of relative cerebral blood flow change by flow-sensitive alternating inversion recovery (FAIR) technique: application to functional mapping. Magn. Reson. Med. 34, 293–301.
Maillard, L., Ishii, K., Bushara, K., Waldvogel, D., Schulman, A.E., Hallett, M., 2000. Mapping the basal ganglia. fMRI evidence for somatotopic representation of face, hand, and foot. Neurology 55, 377–383.
Menon, V., Anagnoson, R.T., Glover, G.H., Pfefferbaum, A., 2000. Basal ganglia involvement in memory-guided movement sequencing. NeuroReport 11, 3641–3645.
Mildner, T., Trampel, R., Moller, H.E., Schafer, A., Wiggins, C.J., Norris, D.G., 2003. Functional perfusion imaging using continuous arterial spin labeling with separate labeling and imaging coils at 3 T. Magn. Reson. Med. 49, 791–795.
Milner, B., 1971. Interhemispheric differences in the localization of psychological processes in man. Br. Med. Bull. 27, 272–277.
Oldfield, R.C., 1970. The assessment and analysis of handedness: the Edinburgh inventory. Neuropsychologia 9, 97–113.
Picard, N., Strick, P.L., 2001. Imaging the premotor areas. Curr. Opin. Neurobiol. 11, 663–672.
Raichle, M.E., MacLeod, A.M., Snyder, A.Z., Powers, W.J., Gusnard, D.A., Shulman, G.L., 2001. A default mode of brain function. Proc. Natl. Acad. Sci. U. S. A. 98, 676–682.
Reddy, H., Matthews, P.M., Lassonde, M., 2000. Functional MRI cerebral activation and deactivation during finger movement. Neurology 55, 1244.
Sadato, N., Campbell, G., Ibanez, V., Deiber, M., Hallett, M., 1996. Complexity affects regional cerebral blood flow change during sequential finger movements. J. Neurosci. 16, 2693–2700.
Sadato, N., Ibanez, V., Campbell, G., Deiber, M.-P., Le Bihan, D., Hallett, M., 1997. Frequency-dependent changes of regional cerebral blood flow during finger movements: functional MRI compared to PET. J. Cereb. Blood. Flow Metab. 17, 670–679.
Sakai, K., Hikosaka, O., Miyauchi, S., Takino, R., Sasaki, Y., Pütz, B., 1998. Transition of brain activation from frontal to parietal areas in visuomotor sequence learning. J. Neurosci. 18, 1827–1840.
Shmuel, A., Yacoub, E., Pfeuffer, J., Van de Moortele, P.F., Adriany, G., Hu, X., Ugurbil, K., 2002. Sustained negative BOLD, blood flow and oxygen consumption response and its coupling to the positive response in the human brain. Neuron 36, 1195–1210.
Silva, A.C., Zhang, W., Williams, D.S., Koretsky, A.P., 1995. Multi-slice MRI of rat brain perfusion during amphetamine stimulation using arterial spin labeling. Magn. Reson. Med. 33, 209–214.
Talagala, S.L., Noll, D.C., 1998. Functional MRI using steady-state arterial water labeling. Magn. Reson. Med. 39, 179–183.
Talagala, S.L., Ye, F.Q., Ledden, P.J., Chesnick, S., 2004a. Whole brain 3D perfusion MRI at 3.0 T using CASL with a separate labeling coil. Magn. Reson. Med. 52, 131–140.
Talagala, S.L., Chuang, K.-H., Chesnick, S., van Gelderen, P., Koretsky, A.P., Duyn, J., 2004b. Abstract. High sensitivity CASL perfusion MRI at 3T using a 16 channel receiver coil array. Proc. ISMRM 11, 717.
Talairach, J., Tournoux, P., 1988. Coplanar stereotaxic atlas of the human brain. 3-Dimensional Proportional System: An Approach to Cerebral Imaging. Thieme Medical, Stuttgart.
Thickbroom, G.W., Byrnes, M.L., Sacco, P., Ghosh, S., Morris, I.T., Mastaglia, F.L., 2000. The role of the supplementary motor area in externally timed movement: the influence of predictability of movement timing. Brain Res. 874, 233–241.
Thieben, M.J., Duggins, A.J., Good, C.D., Gomes, L., Mahant, N., Richards, F., McCusker, E., Frackowiak, R.S., 2002. The distribution of structural neuropathology in pre-clinical Huntington's disease. Brain 125, 1815–1828.
Toni, I., Shah, N.J., Fink, G.R., Thoenissen, D., Passingham, R.E., Zilles, K., 2002. Multiple movement representations in the human brain: an event-related fMRI study. J. Cogn. Neurosci. 14, 769–784.
Wang, J., Alsop, D.C., Li, L., Listerud, J., Gonzalez-At, J.B., Schnall, M.D., Detre, J.A., 2002. Comparison of quantitative perfusion imaging using arterial spin labeling at 1.5 and 4.0 Tesla. Magn. Reson. Med. 48, 242–254.
Wang, J., Aguirre, G.K., Kimberg, D.Y., Roc, A.C., Li, L., Detre, J.A., 2003a. Arterial spin labeling perfusion fMRI with very low task frequency. Magn. Reson. Med. 49, 796–802.
Wang, J., Aguirre, G.K., Kimberg, D.Y., Detre, J.A., 2003b. Empirical analyses of null-hypothesis perfusion FMRI data at 1.5 and 4 T. NeuroImage 19, 1449–1462.
Williams, D.S., Detre, J.A., Leigh, J.S., Koretsky, A.P., 1992. Magnetic resonance imaging of perfusion using spin inversion of arterial water. Proc. Natl. Acad. Sci. U. S. A. 89, 212–216.
Wong, E.C., Buxton, R.B., Frank, L.R., 1997. Implementation of quantitative perfusion imaging techniques for functional brain mapping using pulsed arterial spin labeling. NMR Biomed. 10, 237–249.
Ye, F.Q., Smith, A.M., Yang, Y., Duyn, J., Mattay, V.S., Ruttimann, U.E., Frank, J.A., Weinberger, D.R., McLaughlin, A.C., 1997. Quantitation of

regional cerebral blood flow increases during motor activation: a steady-state arterial spin tagging study. NeuroImage 6, 104–112.

Ye, F.Q., Berman, K.F., Ellmore, T., Esposito, G., Van Horn, J.D., Yang, Y., Duyn, J., Smith, A.M., Frank, J.A., Weinberger, D.R., McLaughlin, A.C., 2000. H(2)(15)O PET validation of steady-state arterial spin tagging cerebral blood flow measurements in humans. Magn. Reson. Med. 44, 450–456.

Yongbi, M.N., Fera, F., Yang, Y., Frank, J.A., Duyn, J.H., 2002. Pulsed arterial spin labeling: comparison of multisection baseline and functional MR imaging perfusion signal at 1.5 and 3.0 T: initial results in six subjects. Radiology 222, 569–575.

Yousry, T.A., Schmid, U.D., Alkadhi, H., Schmidt, D., Peraud, A., Buettner, A., Winkler, P., 1997. Localization of the motor hand area to a knob on the precentral gyrus. A new landmark. Brain 120 (Pt 1), 141–157.

Zaharchuk, G., Ledden, P.J., Kwong, K.K., Reese, T.G., Rosen, B.R., Wald, L.L., 1999. Multislice perfusion and perfusion territory imaging in humans with separate label and image coils. Magn. Reson. Med. 41, 1093–1098.

Zaini, M.R., Strother, S.C., Anderson, J.R., Liow, J.S., Kjems, U., Tegeler, C., Kim, S.G., 1999. Comparison of matched BOLD and FAIR 4.0 T-fMRI with [15O]water PET brain volumes. Med. Phys. 26, 1559–1567.

Zhang, W., Silva, A.C., Williams, D.S., Koretsky, A.P., 1995. NMR measurement of perfusion using arterial spin labeling without saturation of macromolecular spins. Magn. Reson. Med. 33, 370–376.